J Nanostruct 11(1): 73-80, Winter 2021

RESEARCH PAPER

$CuMoO_4$/ ZnO Nanocomposites: Novel Synthesis, Characterization, and Photocatalytic Performance

Rahmad Syah [1], Amjad Hussein Altajer [2], Omar F. Abdul- Rasheed [3], Faisal Amri Tanjung [1,*], Aseel M. Aljeboree [4], Nour Abd Alrazzak [4], Ayad F. Alkaim [4]

[1] *Faculty of Engineering, Medan Area University, Medan, Indonesia*

[2] *Department of pharmaceuticals, College of pharmacy, Almaaqal University, Iraq*

[3] *Department of Chemistry and Biochemistry, College of Medicine, Al- Nahrain University, Baghdad, Iraq*

[4] *Chemistry department, College of science for women, University of Babylon, Iraq*

ARTICLE INFO

Article History:
Received 05 September 2020
Accepted 28 December 2020
Published 01 January 2021

Keywords:
Molybdate
Nanocomposites
Optical properties
Photocatalyst
Water pollutant

ABSTRACT

There are several sources of water contamination. One of the most important pollutant of water is azo dyes-based waste which produced by textile, paper and dye industrials. At this work, the morphological engineered $CuMoO_4$/ ZnO Nanocomposites are prepared via simple and fast hydrothermal-microwave method and applied it as a photocaalyst for degradation of water pollutants. Prepared products is characterized with X-ray diffraction (XRD) analysis, Fourier-transform infrared spectroscopy (FT-IR), Scanning Electron Microscopy (SEM), Ultra violet-Visible (UV-Vis) spectroscopy. The results confirms that size and shape of prepared products is homogenous wih narrow size distribution. In the next step, prepared ZnO, $CuMoO_4$, and ZnO/$CuMoO_4$ nanocomposites were used as catalyst for photodegradation of methylene blue and Rhodamine B. Results showed that ZnO/$CuMoO_4$ nanocomposites have excellent photocatalytic performance. Results indicated that prepared ZnO/$CuMoO_4$ nanocomposites can be degraded 92 and 84% of methylene blue and Rhodamine B under UV irradiation after 70 minutes. The charge transfer from $CuMoO_4$ to ZnO is confirmed by the optical characteristics of ZnO/$CuMoO_4$ nanocomposites. As a result, the potential of electron-hole recombination in $CuMoO_4$ decreases, resulting in holes in the valance band that combine with OH groups on the surface of nanocomposites to form highly reactive OH• radicals. The radicals are damaged when they come into contact with Rhodamine B and Methylene blue.

How to cite this article
Syah S., Altajer A.H., Abdul- Rasheed O.F., Amri Tanjung F., Aljeboree A.M., Abd Alrazzak N., Alkaim A.F. $CuMoO_4$/ ZnO Nanocomposites: Novel Synthesis, Characterization, and Photocatalytic Performance. J Nanostruct, 2021; 11(1): 73-80. DOI: 10.22052/JNS.2021.01.009

INTRODUCTION

Photocatalysts are determined as materials which decompose detrimental substances under the sun lights containing UV rays [1-3]. Since photocatalysts became a viable alternative for pollution control, researchers have worked to improve their reaction rate and photocatalytic activity. Due to their possible applications in solar energy conversion and environmental purification, semiconducting oxide photocatalysts have received a lot of attention in recent years [4-9]. When water comes into contact with a photocatalyst, it creates hydroxyl radicals (•OH) and superoxide ($•O_2$), which are scavenger radicals. These scavenger radicals then destroy organic contaminants in a nonselective manner, degrading them to smaller,

* *Corresponding Author Email: icalamri@gmail.com*

less toxic compounds [10-12].

ZnO is known as one of the most familiar photocatalyst. ZnO-based binary and multiple heterojunction/nanocomposite photocatalysts are gaining a lot of attention due to their potential for solving global energy supply crises and pollutant degradation [13-17]. ZnO has unique optical properties, which helps ZnO to maintain photocatalytic activity at low recombination rates. The optical properties of photocatalyst plays a key role in degradation of pollutants. The photocatalytic application of ZnO nanostructures suffer from different limitations. Till now, various methods have been applied for improvement photocatalytic activity of ZnO nanoparticles, such as doping, and preparing ZnO-based nanocomposites [18-21]. M. Chitra and coworkers measured band gap of ZnO, tin oxide (SnO_2) and vanadium oxide (V_2O_5), their binary and ternary combinations were prepared via hydrothermal route. The unique hierarchical nanostructures of the zinc–tin–vanadium oxide (ZTV) nanocomposite with a larger surface area provided the active surface sites required for ethanol adsorption. ZTV's band gap is calculated to be 1.97 eV. The competing effects of high free carrier concentration and Burstein-Moss shift may be responsible for the band gap narrowing observed in ZTV [22]. Kayode Adesina Adegoke and co-authors prepared ZnO/CdS nanocomposites through two steps via hydrothermal and photochemical method. They found that the composite photodegraded Rhodamine B (RhB) dye azo dye with an efficacy of 85% after 30 minutes under UV irradiation. They reported that CdS/ZnO nanocomposites has better photocatalytic performance than ZnO nanorod [23]. Reda M. Mohamed et al. prepared Ag_2O–ZnO Heterojunctions and applied for photodegradation of tetracycline. They showed that The mesoporous 1.5% Ag_2O–ZnO nanocomposite shows the very best degradation rate among all prepared samples with different ratio, and it had been twenty three and eight orders of magnitudes bigger than those of pristine ZnO NPs and P-25, respectively [24].

In this work, ZnO, $CuMoO_4$, and ZnO/$CuMoO_4$ were prepared via simple and novel method. The prepared samples were characterized via XRD, FTIR, SEM, TEM, and UV-Vis analysis. Then the obtained samples were applied for photodegradation of methylene blue as a water pollutant and compared their efficiency.

MATERIALS AND METHODS

Apparatus and chemicals

Nicolet Magna-550 spectrometer in KBr pellets was connected for recording Fourier change infrared (FT-IR) spectra. Morphological properties of products were examined through filtering electron microscopy (SEM) that gotten on LEO-1455VP prepared with an vitality dispersive X-ray spectroscopy. For in-depth studying of morphological structure, Philips EM208S transmission electron magnifying lens was utilized. X-ray diffraction (XRD) patterns investigation was done by a Philips-X'pertpro, X-ray diffractometer utilizing Ni-filtered Cu Kα radiation. The complete chemicals utilized in this research were of analytical grade: Zinc (Ⅱ) nitrate ($Zn(NO_3)_2.6H_2O$), sodium hydroxide (NaOH), $CuSO_4$, , Polyvinylpyrrolidone (PVP), $(NH_4)_6Mo_7O_{24}.H_2O$, sodium dodecyl sulfate (SDS) from Merck.

Synthesis of ZnO nanoparticle

5M $Zn(NO_3)_2.6H_2O$ was dissolved in 30 ml deionized water. In other beaker, PVP was dissolved in deionized water. The PVP solution was added to Zn^{2+} solution under stirring. Then NaOH solution was added dropwise to obtained solution under stirring until pH=11. After 30 minutes, the solution was transferred to Teflon lined stainless autoclave and heated at 130 °C for 4 h. The as-obtained white precipitate was centrifuged and washed with ethanol and water and dried in 60°C for 12 h.

Synthesis of $CuMoO_4$ nanoparticle

$CuMoO_4$ nanoparticles were prepared via co-precipitation method. 3M $CuSO_4$ and sodium dodecyl sulfate (SDS) were dissolved in deionized water. In other beaker, aqueous solution of $(NH_4)_6Mo_7O_{24}.H_2O$ was prepared. Mo-based solution was added dropwise to Cu-based solution. The solution was heated to 65 °C for 2 h. The obtained greenish precipitate washed and dried in vacuum at 60 °C.

Synthesis of ZnO/$CuMoO_4$ nanoparticle

The prepared ZnO and $CuMoO_4$ nanoparticles were dispersed in ethanol and sonicated for 6 h. Prepared nanocomposites centrifuged and dried at 60 °C for 12 h.

Photocatalytic test

The degradation of methylene blue in aqueous solution was monitored under UV light to

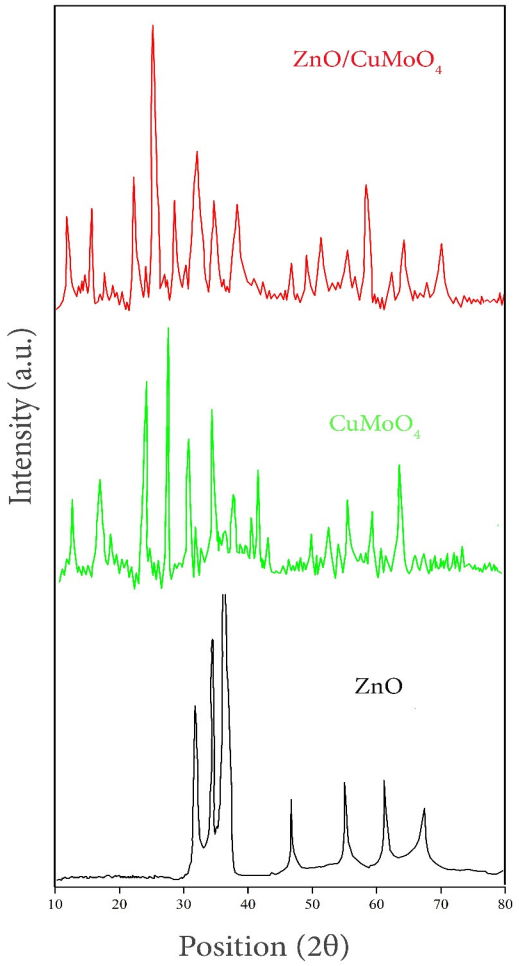

Fig. 1. XRD pattern of as prepared ZnO, $CuMoO_4$ and ZnO/$CuMoO_4$ nanostructures.

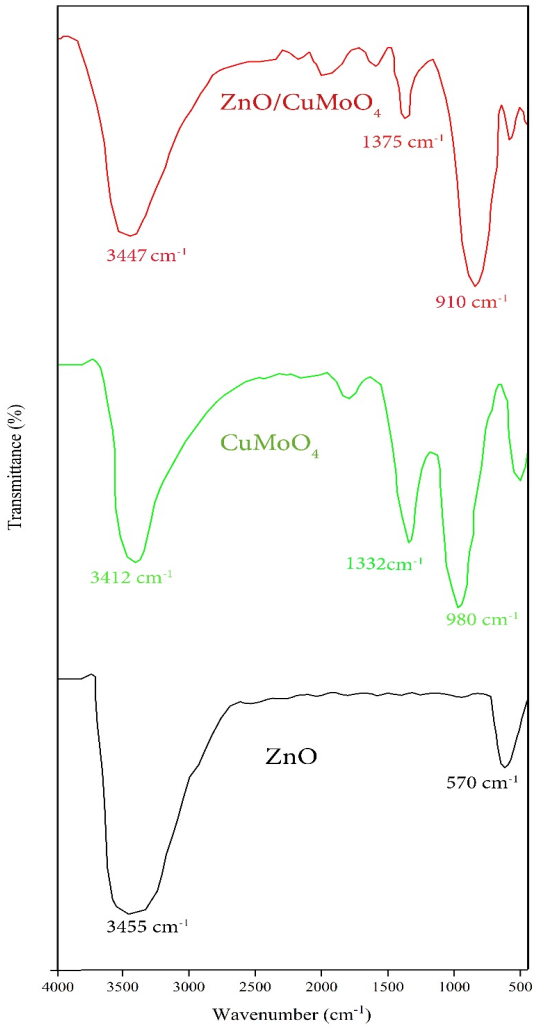

Fig. 2. FT-IR spectrum of synthesized ZnO, $CuMoO_4$ and ZnO/$CuMoO_4$ nanostructures.

determine the photocatalytic activity of prepared samples. In a quartz photocatalytic reactor, the degradation process was carried out. With a 20 ppm dye solution and 0.02 g of samples, photocatalytic degradation was performed. The mixture was then put in a photoreactor under UV light and stirred for 20 minutes in the dark to ensure that the dye molecules on the nanostructures surface were in the proper adsorption-desorption equilibrium needed to serve as an effective photocatalyst. Air was blown into the vessel through a pump to keep the solution oxygen-saturated in the reaction. Then, using 5 minutes of centrifugation at 12,000 rpm, nanoparticles were isolated from the 5cc samples taken from the degraded solution at different time intervals. A UV-vis spectrophotometer was used to calculate the dye concentration.

RESULTS AND DISCUSSION

X-ray diffraction (XRD) was used to describe the phase structure and crystallinity of the prepared products. The XRD pattern of prepared samples is shown in Fig. 1. XRD analysis of a prepared ZnO NPs confirms formation of ZnO (JCPDS: 01-080-0075), $CuMoO_4$ (JCPDS: 31-0449), and ZnO/$CuMoO_4$ nanostructures without any impurity. Scherrer equation [25], $Dc = K\lambda/\beta Cos\theta$, was utilized for crystalline calculation, where β is the width of the observed diffraction peak at its half maximum intensity (FWHM), K is the shape factor, which takes a value of about 0.9, and λ is the X-ray wavelength (CuKα radiation, equals to 0.154 nm). According to Scherrer equation, crystalline size of of ZnO, $CuMoO_4$, and ZnO/$CuMoO_4$ were determined 42, 53, and 48 nm respectively.

Fig. 2 shows FT-IR spectrum of the ZnO, $CuMoO_4$, and ZnO/$CuMoO_4$. For ZnO case, the broad peak from 3100 to 300 cm^{-1} can be attributed to the stretching vibration of the hydrogen bonded OH groups of the surface-adsorbed water. The peak at 570 cm^{-1} is related to the Zn–O bond stretching mode. No other absorption peaks, indicating the purity of the ZnO. For the $CuMoO_4$, the presence of peaks in 1200-1400 cm^{-1} can be related to C-C bond which is related to unwashed SDS. The peak at 800-100 can be assigned to Mo-O-Mo stretching mode. The peaks at CuMoO4, and ZnO/$CuMoO_4$ are confirmed formation metal-oxygen (Zn-O, Mo-O, and Cu-O) bonds.

Scanning electron microscope was applied for morphological investigation of prepared products. Fig. 3a and Fig. 3b presents SEM image of as-prepared ZnO nanoparticles at two magnifications. As well as shown, homogenous nanoparticles with average particle size of 140 nm is formed. For $CuMoO_4$, average particle size was increased to 190 nm (Fig. 3c and Fig. 3d). Fig. 4a and Fig. 4b provides SEM images of ZnO/$CuMoO_4$ nanocomposites. It is clear that particle size of ZnO/$CuMoO_4$ nanocomposites is smaller than ZnO, and $CuMoO_4$ nanoparticles. It can be

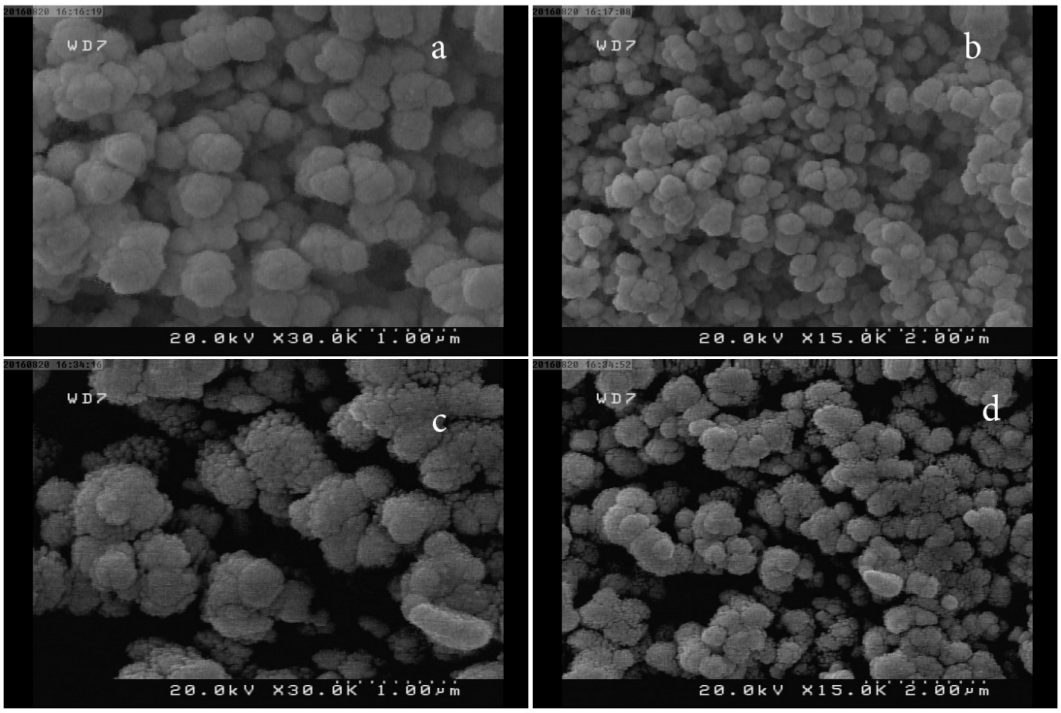

Fig. 3. SEM images of a, b) ZnO and c,d) $CuMoO_4$ nanoparticles with different magnifications.

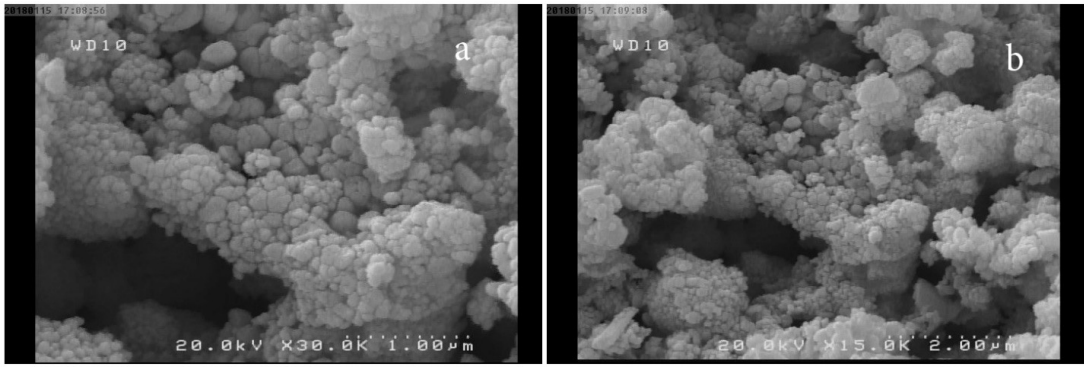

Fig. 4. SEM images of prepared ZnO/$CuMoO_4$ nanocomposites with different magnifications.

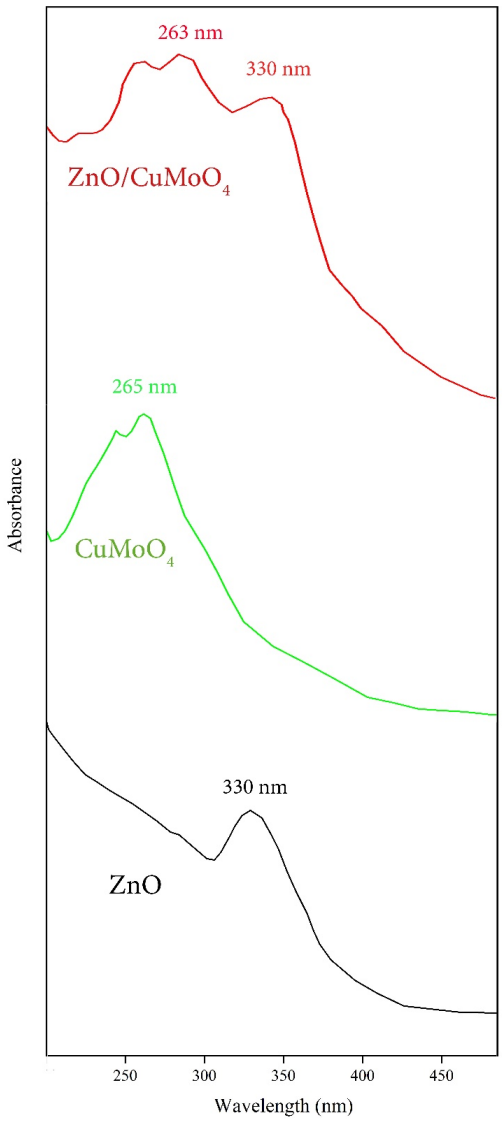

Fig. 5. UV-Vis analysis of as synthesized ZnO, $CuMoO_4$ and ZnO/$CuMoO_4$ nanostructures.

concluded that applied ultrasonic for preparation of ZnO/$CuMoO_4$ separate agglomerated particles and provide smaller particle size.

Fig. 5 shows UV-Vis absorption spectrum of prepared samples. For ZnO NPs, The observable absorption peak at 330 nm asserts the formation of ZnO NPs by the hydrothermal method. In comparison with previously reported papers, there was a considerable blue-shift in the absorption of the prepared ZnO NPs rather than the bulk ZnO. It is clear that there was no impurity-related peak in the spectrum which reveals that synthesized ZnO NPs possess high purity. For $CuMoO_4$ nanoparticles, the absorption spectrum shows a high absorption peak at 268 nm, which is related to Ligand to Metal Charge Transfer (LMCT) from 2p orbitals of oxygen to 4d orbitals of molybdenum inside the MoO_4^{2-} anion.

Recently, azo-dyes included water become a major concern in environmental fields. The prepared nanostructures were applied for photocatalytic investigation. It is concluded from the optical properties which prepared samples can be acted as a good photocatalyst. The present study utilize ZnO, $CuMoO_4$, and ZnO/$CuMoO_4$ for photocatalytic degradation of Rhodamine B and Methylene blue as water pollutants under UV irradiation. Fig. 6 shows photocatalytic

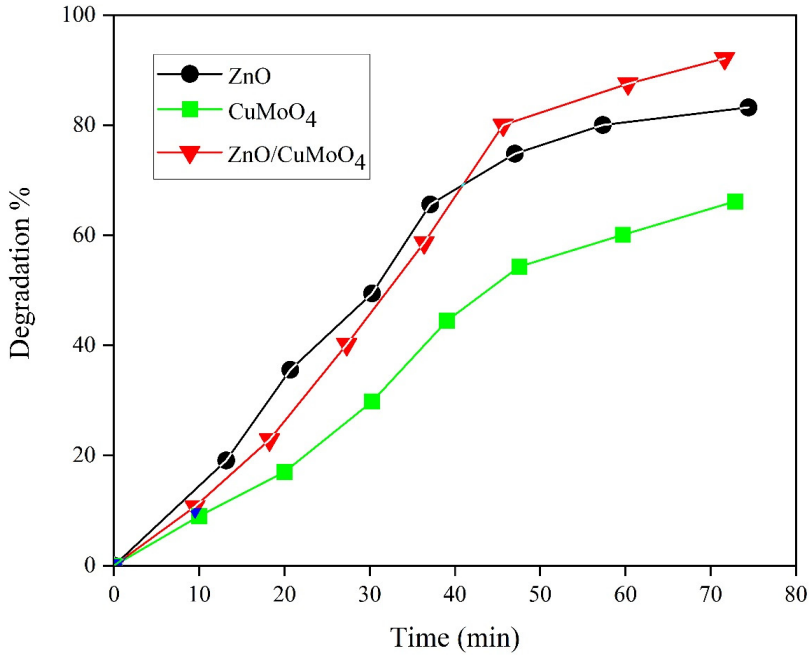

Fig. 6. Photocatalytic activity of ZnO, $CuMoO_4$ and ZnO/$CuMoO_4$ nanocomposite on degradation of Methylene blue under UV irradiation.

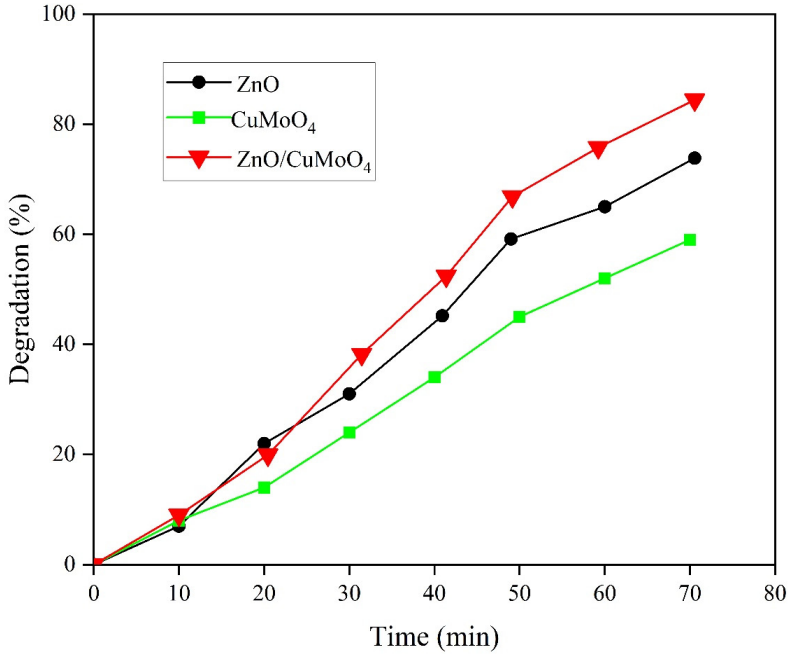

Fig. 7. Photocatalytic activity of ZnO, $CuMoO_4$ and ZnO/$CuMoO_4$ nanocomposite on degradation of Rhodamine B under UV irradiation.

performance of samples for removal of methylene B from water. Results show that ZnO/$CuMoO_4$ nanocomposites degraded 92% of methylene blue after 70 minutes. For ZnO and $CuMoO_4$, the efficiency was measured 74 and 66% respectively. The same results was repeated for photocatalytic degradation of Rhodamine B. As well as shown in Fig. 7, 84% Rhodamine B was degraded after 70 minutes UV irradiation. The photocatalytic efficiency was measured 59, and 73% for $CuMoO_4$

and ZnO respectively. The optical properties of ZnO/$CuMoO_4$ nanocomposites confirms the charge transfer from $CuMoO_4$ to ZnO. So, recombination of electron-hole possibility in $CuMoO_4$ becomes small and create holes in valance band react with OH groups on the surface of nanocomposites and cause to produce highly reactive OH• radicals. As-produced radicals react with Rhodamine B and Methylene blue and degraded. In overall, results introduce high potentially ZnO/$CuMoO_4$ nanocomposites as a photocatalytic degradant of water pollutants.

CONCLUSION

In summary, the ZnO, $CuMoO_4$ and ZnO/$CuMoO_4$ nanostructures were prepared via hydrothermal, co-precipitation, and ultrasonic-assisted routes respectively. The prepared samples were characterized via XRD, FTIR, FESEM, and UV-Vis analysis. The attractive optical properties of prepared samples lead to application of products in photocatalytic process. So, prepared nanostructures were applied for photocatalytic degradation of azo dyes as water pollutants. It is found that prepared ZnO/$CuMoO_4$ nanocomposites has a high potential for removal Methylene blue and Rhodamine B from water. The results revealed that 92 and 84% of methylene blue and Rhodamine B were degraded after 70 minutes respectively.

CONFLICT OF INTEREST

The authors declare that there is no conflict of interests regarding the publication of this manuscript.

REFERENCES

1. Sagir M, Tahir MB, Waheed U. Role of Photocatalysts in Organic Pollutants Degradation. Reference Module in Materials Science and Materials Engineering: Elsevier; 2020.
2. Sakka S. Chapter 11.1.2 - Sol–Gel Process and Applications. In: Somiya S, editor. Handbook of Advanced Ceramics (Second Edition). Oxford: Academic Press; 2013. p. 883-910.
3. Yang X, Wang D. Photocatalysis: From Fundamental Principles to Materials and Applications. ACS Applied Energy Materials. 2018;1(12):6657-93.
4. Tang G, Abas A, Wang S. Photocatalytic Degradation and Hydrogen Production of TiO_2/Carbon Fiber Composite Using Bast as a Carbon Fiber Source. International Journal of Photoenergy. 2018;2018.
5. Xing P, Chen P, Chen Z, Hu X, Lin H, Wu Y, Zhao L, He Y. Novel ternary MoS_2/C-ZnO composite with efficient performance in photocatalytic NH_3 synthesis under simulated sunlight. ACS Sustainable Chemistry & Engineering. 2018;6(11):14866-79.
6. Mohd Adnan MA, Phoon BL, Muhd Julkapli N. Mitigation of pollutants by chitosan/metallic oxide photocatalyst: A review. Journal of Cleaner Production. 2020;261:121190.
7. Zhang G, Zhang X, Meng Y, Pan G, Ni Z, Xia S. Layered double hydroxides-based photocatalysts and visible-light driven photodegradation of organic pollutants: A review. Chemical Engineering Journal. 2020;392:123684.
8. Police AKR, Vattikuti SVP, Mandari KK, Chennaiahgari M, M.V PS, Valluri DK, et al. Bismuth oxide cocatalyst and copper oxide sensitizer in $Cu_2O/TiO_2/Bi_2O_3$ ternary photocatalyst for efficient hydrogen production under solar light irradiation. Ceramics International. 2018;44(10):11783-91.
9. Chen Q, Cheng X, Long H, Rao Y. A short review on recent progress of Bi/semiconductor photocatalysts: The role of Bi metal. Chinese Chemical Letters. 2020;31(10):2583-90.
10. Kurenkova AY, Markovskaya DV, Gerasimov EY, Prosvirin IP, Cherepanova SV, Kozlova EA. New insights into the mechanism of photocatalytic hydrogen evolution from aqueous solutions of saccharides over CdS-based photocatalysts under visible light. International Journal of Hydrogen Energy. 2020;45(55):30165-77.
11. Xia P, Zhu B, Cheng B, Yu J, Xu J. 2D/2D g-C_3N_4/MnO_2 nanocomposite as a direct Z-scheme photocatalyst for enhanced photocatalytic activity. ACS Sustainable Chemistry & Engineering. 2018;6(1):965-73.
12. Obregón S, Zhang Y, Colón G. Cascade charge separation mechanism by ternary heterostructured $BiPO_4/TiO_2$/g-C_3N_4 photocatalyst. Applied Catalysis B: Environmental. 2016;184:96-103.
13. Serrà A, Pip P, Gómez E, Philippe L. Efficient magnetic hybrid ZnO-based photocatalysts for visible-light-driven removal of toxic cyanobacteria blooms and cyanotoxins. Applied Catalysis B: Environmental. 2020;268:118745.
14. Tekin D, Kiziltas H, Ungan H. Kinetic evaluation of ZnO/TiO_2 thin film photocatalyst in photocatalytic degradation of Orange G. Journal of Molecular Liquids. 2020;306:112905.
15. Gang R, Xu L, Xia Y, Cai J, Zhang L, Wang S, et al. Fabrication of MoS_2 QDs/ZnO nanosheet 0D/2D heterojunction photocatalysts for organic dyes and gaseous heavy metal removal. Journal of Colloid and Interface Science. 2020;579:853-61.
16. Zhu P, Hu M, Duan M, Xie L, Zhao M. High visible light response Z-scheme Ag_3PO_4 / g-C_3N_4 / ZnO composite photocatalyst for efficient degradation of tetracycline hydrochloride: Preparation, properties and mechanism. Journal of Alloys and Compounds. 2020;840:155714.
17. Roy N, Chakraborty S. ZnO as photocatalyst: An approach to waste water treatment. Materials Today: Proceedings. 2020.
18. Elsayed MH, Elmorsi TM, Abuelela AM, Hassan AE, Alhakemy AZ, Bakr MF, et al. Direct sunlight-active Na-doped ZnO photocatalyst for the mineralization of organic pollutants at different pH mediums. Journal of the Taiwan Institute of Chemical Engineers. 2020;115:187-97.
19. Ahmad I, Akhtar MS, Ahmed E, Ahmad M. Highly efficient visible light driven photocatalytic activity of graphene and CNTs based Mg doped ZnO photocatalysts: A comparative study. Separation and Purification Technology. 2020;245:116892.

20. Ahmad I. Comparative study of metal (Al, Mg, Ni, Cu and Ag) doped ZnO/g-C_3N_4 composites: Efficient photocatalysts for the degradation of organic pollutants. Separation and Purification Technology. 2020;251:117372.
21. Gonzalez-Casamachin DA, Rivera De la Rosa J, Lucio–Ortiz CJ, Sandoval-Rangel L, García CD. Partial oxidation of 5hydroxymethylfurfural to 2,5-furandicarboxylic acid using O2 and a photocatalyst of a composite of ZnO/PPy under visible-light: Electrochemical characterization and kinetic analysis. Chemical Engineering Journal. 2020;393:124699.
22. Chitra M, Mangamma G, Uthayarani K, Neelakandeswari N, Girija EK. Band gap engineering in ZnO based nanocomposites. Physica E: Low-dimensional Systems and Nanostructures. 2020;119:113969.
23. Adegoke KA, Iqbal M, Louis H, Bello OS. Synthesis, characterization and application of CdS/ZnO nanorod heterostructure for the photodegradation of Rhodamine B dye. Materials Science for Energy Technologies. 2019 Aug 1;2(2):329-36.
24. Mohamed RM, Ismail AA, Kadi MW, Alresheedi AS, Mkhalid IA. Facile Synthesis of Mesoporous Ag_2O–ZnO Heterojunctions for Efficient Promotion of Visible Light Photodegradation of Tetracycline. ACS omega. 2020;5(51):33269-79.
25. Esmaeili-Bafghi-Karimabad A, Ghanbari D, Salavati-Niasari M, Safardoust-Hojaghan H. Microwave-assisted synthesis of SiO_2 nanoparticles and its application on the flame retardancy of poly styrene and poly carbonate nanocomposites. Journal of Nanostructures. 2015;5(3):263-269.